Cluster spin-glass behavior and memory effect in $Cr_{0.5}Fe_{0.5}Ga$

Pallab Bag, P. R. Baral, and R. Nath*

School of Physics, Indian Institute of Science Education and Research Thiruvananthapuram, Kerala-695016, India

(Received 22 September 2017; revised manuscript received 7 September 2018; published 26 October 2018)

We report the structural, static, and dynamic properties of $Cr_{0.5}Fe_{0.5}Ga$ by means of powder x-ray diffraction, dc magnetization, heat capacity, ac susceptibility, magnetic relaxation, and magnetic memory effect measurements. The dc magnetization and ac susceptibility studies reveal a spin-glass transition at around $T_f \simeq 22$ K. An intermediate value of the relative shift in freezing temperature $\delta T_f \simeq 0.017$, obtained from the ac susceptibility data reflects the formation of cluster spin-glass states. The frequency dependence of T_f is also analyzed within the framework of dynamic scaling laws such as power law and Vogel-Fulcher law. The analysis using power law yields a characteristic time constant for a single spin flip $\tau* \simeq 1.1 \times 10^{-10}$ s and critical exponent $z\nu' = 4.2 \pm 0.2$. On the other hand, the Vogel-Fulcher law yields the characteristic time constant for a single spin flip $\tau_0 \simeq 6.6 \times 10^{-9}$ s, Vogel-Fulcher temperature $T_0 = 21.1 \pm 0.1$ K, and an activation energy $E_a/k_B \simeq 16$ K. The value of $\tau*$ and τ_0 along with a nonzero value of T_0 provide further evidence for the cluster spin-glass behavior. The magnetic field dependent T_f follows the de Almeida-Thouless (AT) line with a non-mean-field type instability, reflecting either a different universality class or strong anisotropy in the spin system. A detailed nonequilibrium dynamics study via relaxation and memory effect experiments demonstrates the evolution of the system through a number of intermediate metastable states and striking memory effects. All the above observations render a cluster spin-glass behavior in $Cr_{0.5}Fe_{0.5}Ga$, which is triggered by magnetic frustration due to competing antiferromagnetic and ferromagnetic interactions and magnetic site disorder. Moreover, the asymmetric response of magnetic relaxation with respect to the change in temperature, below the freezing temperature can be explained by the hierarchical model.

DOI: 10.1103/PhysRevB.98.144436

I. INTRODUCTION

In the past years, alloys showing spin-glass (SG) behavior have been widely pursued in order to study exchange bias effect, slow dynamics, memory effect, aging effect, etc. [1–8]. SG is basically a disordered ground state where the spins are frozen along arbitrary direction, below a critical temperature. It is commonly believed that SG appears in systems where magnetic long-range-ordering (LRO) is disturbed by site disorder and magnetic frustration [2,3]. Examples of such systems include metallic SGs where magnetic impurities are randomly diluted in a nobel metal, geometrically frustrated lattices where lattice topology precludes the minimization of energy, systems frustrated due to competing antiferromagnetic (AFM) and ferromagnetic (FM) interactions or competing nearest neighbor and next nearest neighbor interactions, etc. [9,10]. SG-like nonequilibrium dynamics has been observed in several systems where the basic building blocks responsible for the glassy behavior are bigger spin entities, rather than individual spins, referred as "spin clusters." Such systems are often characterized by slow dynamics, similar to the classical SGs. Despite an extensive study on SGs, a consensus about the ground state and dynamics in these systems is still lacking. Here, we report the magnetic studies on the diluted alloy $Cr_{0.5}Fe_{0.5}Ga$ which exhibits features that are reminiscent of cluster SG.

The isostructural alloys CrGa and FeGa crystallize in a Cr_5Al_8-type rhombohedral structure (space group $R\bar{3}m$) with lattice constants [$a = 12.625(8)$ Å and $c = 7.785(10)$ Å] and [$a = 12.4368(11)$ Å and $c = 7.7642(10)$ Å], respectively [11]. In the unit cell, both Ga and Cr/Fe occupy three inequivalent sites each. They form two types of icosahedra: one is Ga-centered and the other one is Cr/Fe-centered, which are alternating along the crystallographic c-direction forming chains. Magnetic susceptibility of CrGa is almost temperature independent while for FeGa, it shows a peak at ~42 K and a broad maximum at ~135 K. Band structure calculations predict weak AFM and dominant FM exchange couplings for CrGa and FeGa, respectively [11]. Therefore substitution of Fe at the Cr site in CrGa can alter the AFM interaction among the Cr atoms and induce different magnetic states. Ko *et al.* tried to synthesize $Cr_{1-x}Fe_xGa$ for different values of x but they succeeded to synthesize phase pure sample only for $x = 0.5$ [12]. Neutron powder diffraction on $Cr_{0.5}Fe_{0.5}Ga$ revealed average composition of the powder sample to be $Cr_{0.515}Fe_{0.485}Ga$ with lattice constants $a = 12.5448(4)$ Å and $c = 7.8557(2)$ Å at room temperature and partial ordering of Cr and Fe atoms among three crystallographic sites. In particular, the Cr and Fe atoms occupy three inequivalent sites: M1(3b), M2(18h), and M3(18h). The refined site occupancies for Cr/Fe are 0.587/0.413, 0.636/0.364, and 0.383/0.617, respectively. Preliminary magnetization measurements suggest the onset of a magnetic ordering at $T \simeq 25$ K. Subsequent theoretical calculations indicated that the Fe-Fe and Cr-Fe interactions are FM and AFM, respectively with an overall

*rnath@iisertvm.ac.in

ferrimagnetic ordering at low temperature [12]. However, a clear understanding of the ground state properties of this alloy requires a detailed experimental investigation which is not yet done.

In this work, we carried out a comprehensive study of the structural and magnetic properties of $Cr_{0.5}Fe_{0.5}Ga$. The 50 % Fe substitution at the Cr site induces atomic disorder in the lattice, preserving the original crystal structure. It is found to be a magnetically frustrated system which undergoes a SG transition at low temperatures. The dc magnetization along with the ac susceptibility data render the system a cluster SG-type. Finally, the magnetic memory effect in the system has been demonstrated by the magnetic relaxation and memory effect measurements.

II. EXPERIMENTAL DETAILS

Polycrystalline $Cr_{0.5}Fe_{0.5}Ga$ sample was synthesized by the conventional solid state reaction technique, taking the constituent elements in the desired stoichiometry. The elements (Fe, Cr, and Ga) used here are of high pure (99.99%) obtained from Sigma Aldrich. The stoichiometric amounts were sealed in a quartz tube in Ar atmosphere. The ampoule was first heated at 1050 °C for 3 days and then at 850 °C for 5 days. The powder x-ray diffraction (XRD) measurements were carried out (PANalytical powder diffractometer with Cu K_α radiation) as a function of temperature using a low-temperature attachment (Oxford Phenix). The dc and ac magnetization (M) measurements were performed using a vibrating sample magnetometer (VSM) attachment to the physical property measurement system (PPMS, Quantum Design). Heat capacity (C_p) was measured using the heat capacity option in the PPMS, adopting the relaxation technique.

III. RESULTS AND DISCUSSION

A. X-ray diffraction

In order to confirm the phase purity and to detect the structural transition, if any, powder XRD was measured at different temperatures. Rietveld refinement of the XRD pattern was carried out using the FULLPROF package [13]. The initial structural parameters for this purpose were taken from Ref. [11]. Figure 1 shows the Rietveld refinement of the powder XRD pattern at 300 and 15 K. A good fitting of the room temperature data with a reduced value of goodness-of-fit ($\chi^2 \simeq 2.8$) suggests that the sample is phase pure. The obtained lattice constants at room temperature are $a = 12.544(4)$ Å and $c = 7.853(2)$ Å, which are consistent with the previous report [12]. Figure 2 displays the temperature variation of lattice constants and unit cell volume (V_{cell}). No structural transition was observed down to 15 K and the lattice constants and V_{cell} were found to decrease systematically with decreasing temperature. The temperature variation of V_{cell} was fitted by the equation [14]

$$V_{cell}(T) = \gamma U(T)/K_0 + V_0, \tag{1}$$

where V_0 is the cell volume at $T = 0$ K, K_0 is the bulk modulus, and γ is the Grüneisen parameter. $U(T)$ is the internal energy, which can be expressed in terms of the Debye

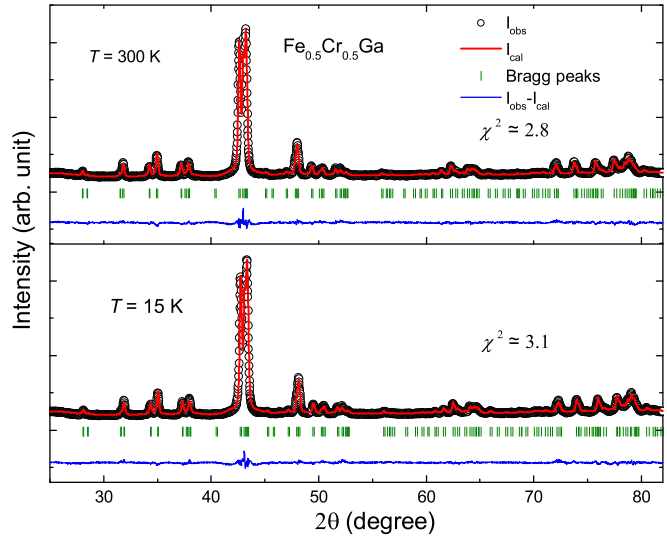

FIG. 1. Rietveld refinement of the x-ray diffraction pattern of $Cr_{0.5}Fe_{0.5}Ga$ at $T = 300$ (top) and 15 K (bottom), respectively. The open circles and solid lines are the observed and calculated patterns, respectively. The Bragg positions are indicated by ticks. Solid line at the bottom represents the difference between the observed and calculated intensities.

approximation as

$$U(T) = 9pk_BT\left(\frac{T}{\theta_D}\right)^3 \int_0^{\theta_D/T} \frac{x^3}{e^x - 1}dx. \tag{2}$$

Here, p is the number of atoms in the specimen and k_B is the Boltzmann constant. Using this approximation (see the fit in the lower panel of Fig. 2), the Debye temperature (θ_D) for $Cr_{0.5}Fe_{0.5}Ga$ was estimated to be $\theta_D \simeq 350$ K.

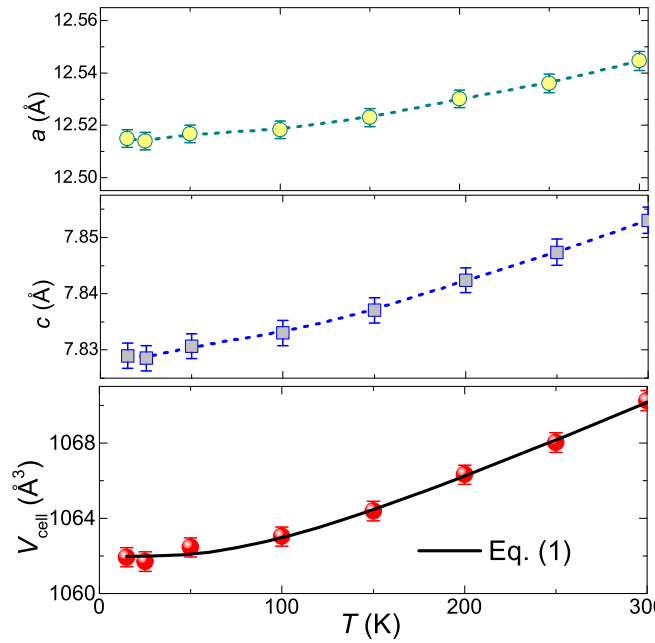

FIG. 2. Variation of lattice constants (a and c) and unit cell volume (V_{cell}) with temperature for $Cr_{0.5}Fe_{0.5}Ga$. The solid line represents the fit of $V_{cell}(T)$ using Eq. (1).

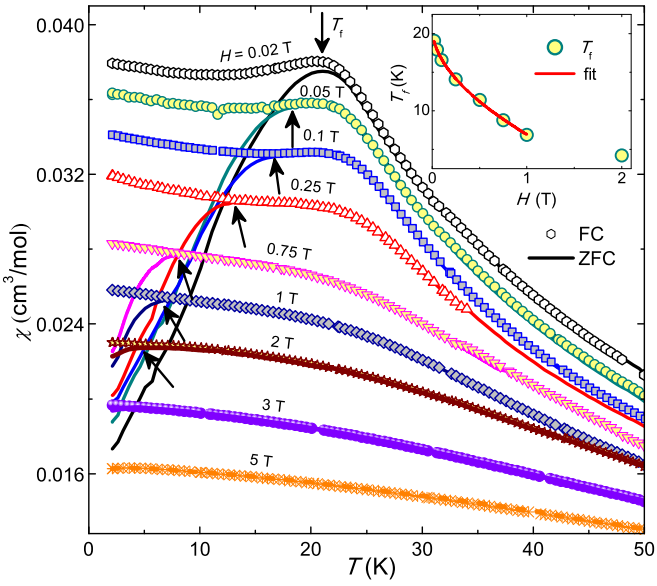

FIG. 3. Temperature dependent dc susceptibility $\chi(T)$ measured under different applied fields for ZFC and FC protocols. The arrows point to T_f. Inset: The variation of T_f with H. The solid line represents the fit using Eq. (4).

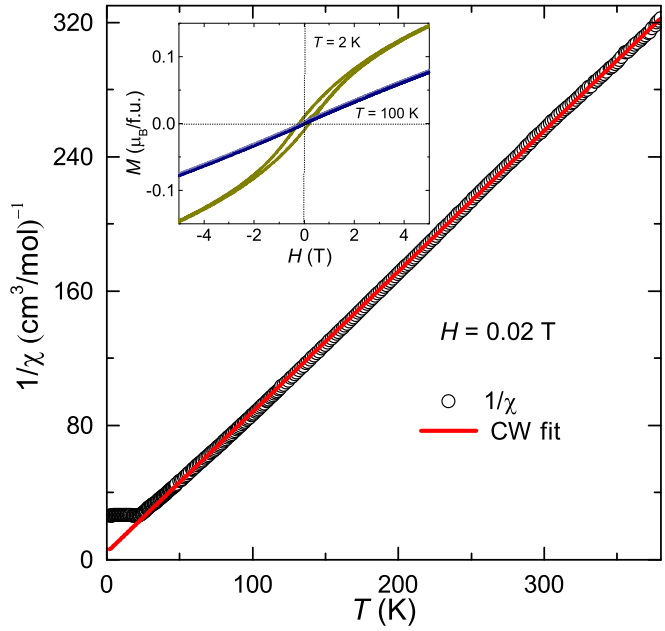

FIG. 4. $1/\chi$ vs T measured at $H = 0.02$ T and the solid line is the CW fit for $T > 50$ K. Inset: Isothermal magnetization $M(H)$ curves at $T = 2$ K and 100 K.

B. DC magnetization

Figure 3 presents the temperature dependent dc susceptibility, $\chi(T)$ ($\equiv M/H$) measured in different applied fields (H), during heating after zero-field-cooled (ZFC) and field-cooled (FC) conditions. For $H = 0.02$ T, both ZFC and FC data show a broad peak and a bifurcation at the same temperature possibly suggesting a glass transition around 22 K. The temperature at which the bifurcation occurs is called the freezing temperature, denoted as T_f. In order to elucidate the nature of the transition, we measured $\chi(T)$ at different applied fields for ZFC and FC protocols. As the field increases, the absolute value of χ decreases systematically and the ZFC data develop a plateau with two broad edges on either side. The low temperature edge corresponding to T_f shifts towards lower temperatures while the edge at the high temperature side shifts towards higher temperatures. Furthermore, the difference between ZFC and FC curves ($\Delta\chi$) at low temperatures decreases with increasing magnetic field. The shifting of T_f towards lower temperatures and the reduction in $\Delta\chi$ indicate the frozen spin-glass (SG) state below T_f [3]. For the field above 3 T, T_f is suppressed below 2 K and hence not detectable. The shifting of high temperature edge towards high temperatures with field appears to be due to the onset of a magnetic LRO. However, our heat capacity measurement (discussed later) rules out any magnetic ordering at this temperature. The overall behavior of $\chi(T)$ is nearly similar to that reported for SG compound U_2PdSi_3 [15].

Magnetic isotherm [$M(H)$] measurements were also performed at different temperatures (inset of Fig. 4). At high temperatures, $M(H)$ is nearly straight line, as expected in the paramagnetic (PM) region. With decreasing temperature, it develops a curvature which is more pronounced at low temperatures. At the lowest measured temperature of $T = 2$ K, it shows a small hysteresis with a coercive field of ∼200 Oe. However, the value of magnetization even at 9 T (not shown) is much less than the saturation value expected for this alloy. A weak hysteresis and the reduced value of magnetization at 9 T exclude the possibility of a FM/ferrimagnetic transition and establishes low temperature SG behavior of the compound [3,16].

As shown in Fig. 4, the inverse susceptibility $1/\chi$ (measured at $H = 0.02$ T) in the high temperature regime ($T >$ 50 K) is fitted by the Curie-Wiess (CW) law

$$\chi = \frac{C}{T - \theta_{CW}}, \tag{3}$$

where C and θ_{CW} represent the Curie constant and CW temperature, respectively. The obtained values are $C \simeq 1.2\ \mathrm{cm^3\ K\ mol^{-1}}$ and $\theta_{CW} \simeq -5$ K. The negative value of θ_{CW} signifies the presence of dominant AFM interaction in the system. From the value of C, the effective magnetic moment μ_{eff} ($= \sqrt{3k_B C/N_A}$, where N_A is the Avogadro's number) was calculated to be $\sim 3.1\mu_B$. In spin systems, according to the mean-field theory θ_{CW} represents the sum of all the exchange couplings. Our estimated value of θ_{CW} is much smaller compared to T_f, which possibly reflects that the system is frustrated due to competing AFM and FM interactions [17], as anticipated from the previous theoretical calculations [12]. In addition to the magnetic site disorder, this competing interactions is also responsible for the low temperature SG behavior of the system.

The variation of T_f with H in the low-field region is presented in the inset of Fig. 3. It decreases systematically with increasing field, consistent with the SG transition. In the H-T phase diagram for SG systems, typically, two irreversible lines are observed: Gabay-Toulouse (GT) line ($T_f \propto H^2$) and de Almeida-Thouless (AT) line [18,19]. The AT line marks the PM to SG transition, which is usually observed

for Ising spin systems. On the other hand, in the case of Heisenberg spin systems, both the lines are expected. In the strong anisotropy (strong irreversibility) regime, the system is Ising-type and the line follows AT character, whereas in the weak anisotropy regime, the line corresponds to GT line. A quantitative difference is expected in the behavior of AT line in the mean-field and non-mean-field scenarios. According to the non-mean-field scaling theory, the variation of T_f with H in the low-field region follows [20]:

$$T_f(H) = T_f(0)(1 - AH^{2/\Phi}), \quad (4)$$

where A is the amplitude, $T_f(0)$ is the value of T_f in the absence of a magnetic field, and Φ is the crossover exponent. In the mean-field model, it has a value $\Phi = 3$. In our system, only one irreversible line was observed which could be fitted by Eq. (4). As shown in the inset of Fig. 3, the best fit was obtained for $H < 1$ T with $T_f(0) \simeq 20.7$ K and $\Phi \simeq 3.8$. This value of Φ is larger than the one expected for the AT line with mean-field instability [19]. In several SG systems such as Nd_2AgIn_3(Ref. [21]), U_2IrSi_3 (Ref. [22]), $Zn_3V_3O_8$ (Ref. [23]), Nd_5Ge_3 (Ref. [24]), $LiMn_2O_4$ (Ref. [25]), etc., the authors have reported a mean-field type behavior.[1] An analysis (reported in Ref. [26,27]) in terms of non-mean-field model [Eq. (4)] on a group of SG systems resulted in a large variation of Φ from 5 for the canonical Heisenberg SG system MnCu to 3.2 for the random-anisotropy SG system a-DyNi, suggesting that they all do not belong to the same universality class. This model has also been tested on other SG systems, which produces a non-mean-field-type exponent [28–30]. The obtained value of $\Phi \simeq 3.8$ for our system falls in the intermediate range, reflecting either a different universality class or role of dominant anisotropy in the system.

C. Heat capacity

Figure 5 shows the temperature dependent C_p in the absence of magnetic field. No anomaly associated with the magnetic LRO was observed down to 2 K. The value of C_p at $T = 250$ K is about 48.2 J mol^{-1} K^{-1}, which is close to the expected Dulong-Petit value $C_v = 3mR = 6R =$ 49.8 J mol^{-1} K^{-1}, where R is the gas constant and m is the number of atoms per formula unit. In an attempt to check whether one can fit the data in the low-temperature region by $C_p(T) = \gamma T + \beta T^3$, C_p/T versus T^2 is plotted in the lower inset of Fig. 5. Here, γ is the Sommerfeld coefficient which represents the electronic contribution and β represents the lattice contribution. It clearly shows a nonlinear behavior. However, the low-temperature C_p data could be fitted well by adding a magnetic term $\delta T^{3/2}$ in $C_p(T) = \gamma T + \beta T^3$, i.e., $C_p(T) = \gamma T + \beta T^3 + \delta T^{3/2}$, where δ is the coefficient of $T^{3/2}$ [31]. A $T^{3/2}$ term in C_p is typical for SG and FM systems [32]. The best fit of the data in the temperature range 2–10 K (upper inset of Fig. 5) yields $\gamma \simeq 29$ mJ mol^{-1} K^{-2}, $\beta \simeq 0.072$ mJ mol^{-1} K^{-4}, and $\delta \simeq 0.7$ mJ mol^{-1} K$^{-5/2}$. From the values of β, one can calculate the Debye temperature (θ_D)

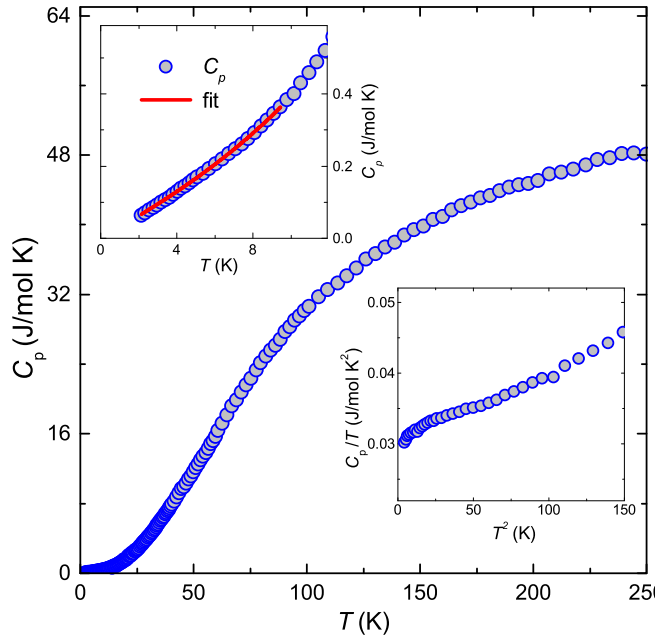

FIG. 5. Temperature dependent heat capacity C_p in the absence of magnetic field between 2 and 250 K. Lower inset: C_p/T vs T^2. Upper inset: C_p vs T in the low temperatures regime and solid line is the fit in the temperature range 2 to 10 K, as described in the text.

using the standard expression $\theta_D = (12\pi^4 mR/5\beta)^{1/3}$. The value of θ_D is calculated to be ~377 K, which is close to the value obtained from the V_{cell} versus T analysis. A large value of γ is reported for several cluster SG systems but the effect of disorder on the density of states is not yet understood [15,31,33].

D. AC susceptibility

In order to understand the underlying nature of the transition and to study the dynamics of the SG state, ac susceptibility was measured at different frequencies (ν) and at a fixed excitation field of $H_{ac} = 5$ Oe, after cooling the sample in zero field. The real part of the ac susceptibility (χ') as a function of temperature is plotted in the upper panel of Fig. 6. It exhibits a pronounced anomaly at around 22.5 K (for $\nu = 200$ Hz), which is found to be frequency dependent. The peak position shifts towards higher temperatures and the height of the peak decreases with increasing ν, consistent with a glassy transition with freezing temperature $T_f \simeq 22.5$ K. ac susceptibility was also measured under different dc fields (H_{dc}) fixing the ac excitation at $H_{ac} = 5$ Oe and $\nu = 200$ Hz. As one can see in the lower panel of Fig. 6, the peak at $T_f \simeq 22.5$ K in zero-field transforms into a broad shoulder like shape when H_{dc} is applied, similar to the dc susceptibility data. With increasing H_{dc}, the low temperature edge (T_f) moves towards low temperatures, further supporting the SG transition. The variation of T_f with H could also be fitted well using Eq. (4) (see the inset of Fig. 6), which yields $T_f(0) \simeq 22.7$ K and $\Phi \simeq 3.6$. The obtained value of Φ again reflects the de Almeida-Thouless line with non-mean-field instability.

[1]In these experimental papers, the authors have force-fitted their data to a mean-field model rather than attempting a more general non-mean-field-type model.

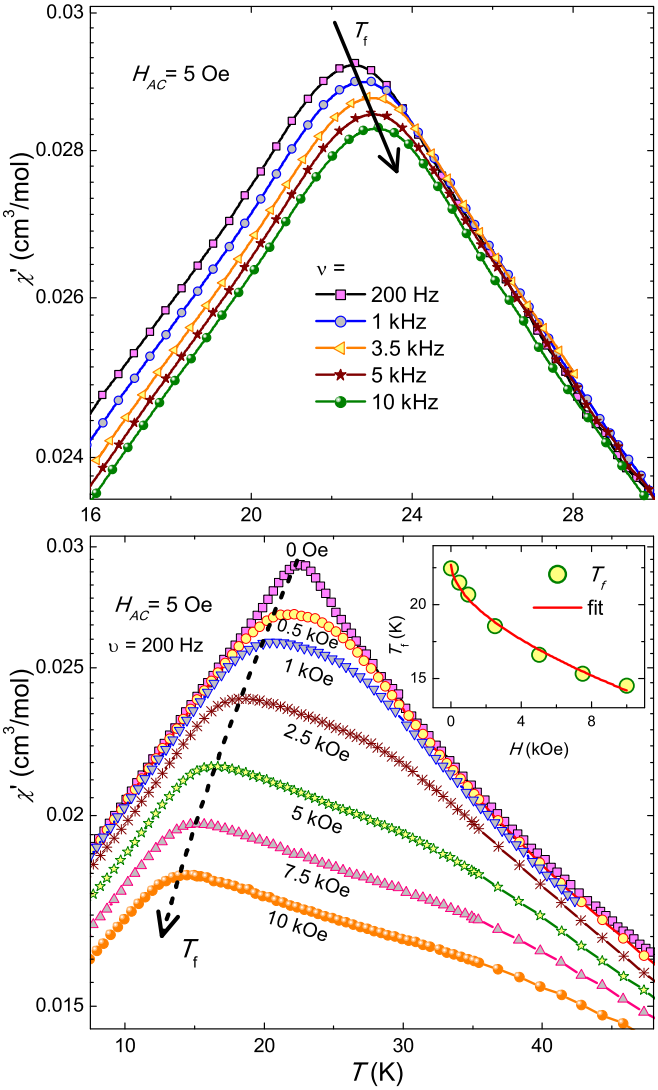

FIG. 6. Upper panel: Real part of the ac susceptibility $[\chi'(T)]$ measured at different frequencies (ν) and at an ac field $H_{ac} = 5$ Oe. The solid downward arrow points to the peak shift. Lower panel: $\chi'(T)$ measured at different dc applied fields, fixing $\nu = 200$ Hz and $H_{ac} = 5$ Oe. The dotted downward arrow guides the peak position. Inset: The variation of T_f with H. The solid line represents the fit using Eq. (4).

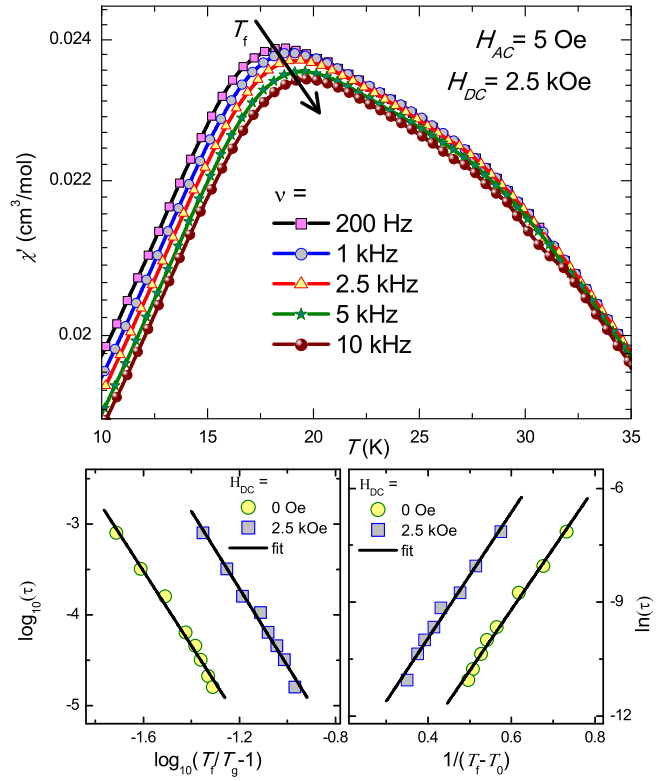

FIG. 7. Upper panel: $\chi'(T)$ measured at different frequencies (ν) at a fixed dc field $H_{dc} = 0.25$ T and at a fixed ac field $H_{ac} = 5$ Oe. The downward arrow points to the peak shift. Lower left panel: $\log_{10}(\tau)$ vs $\log_{10}(T_f/T_g - 1)$ for $H_{dc} = 0$ and 0.25 T. The solid lines represent the fits using Eq. (7). Lower right panel: $\ln(\tau)$ vs $1/(T_f - T_0)$ for $H_{dc} = 0$ and 0.25 T. The solid lines represent the fits using Eq. (10).

For the sake of completeness, we measured ac susceptibility at different frequencies for a fixed dc field of 0.25 T and a fixed ac field of 5 Oe. As shown in the upper panel of Fig. 7, χ' manifests a peak at T_f, which moves towards high temperatures and the magnitude of χ' decreases with increasing frequency. The increase in T_f with ν again supports the SG behavior of the system.

The relative shift in freezing temperature (δT_f) per decade of frequency is often used as a parameter to compare different SG systems. We calculated this parameter using the relation [2,34]

$$\delta T_f = \frac{\Delta T_f}{T_f \Delta(\log_{10} \nu)}, \tag{5}$$

where $\Delta T_f = (T_f)_{\nu_1} - (T_f)_{\nu_2}$ and $\Delta \log_{10}(\nu) = \log_{10}(\nu_1) - \log_{10}(\nu_2)$. δT_f is also known as the Mydosh parameter [35]. For this purpose, two outermost frequencies, $\nu_1 = 200$ Hz and $\nu_2 = 10$ kHz were employed. For our system, this value is calculated to be $\delta T_f \simeq 0.017$, using the data shown in the upper panel of Fig. 7. It is about an order of magnitude larger than the values reported for canonical SG systems such as AuMn ($\delta T_f = 0.0045$) [34] and CuMn ($\delta T_f = 0.005$) [2] and one order of magnitude smaller than what is expected for superparamagnets (e.g., for the ideal noninteracting superparamagnetic system α-$[Ho_2O_3(B_2O_3)]$, $\delta T_f \simeq 0.28$) [2]. In fact, this value is in the range usually observed for cluster SG, categorizing our system as a cluster-SG type [2,23–25,31]. The value of δT_f essentially reflects the response or sensitivity to frequency which strongly depends on the interaction between the underlying entities. In case of magnetic clusters, the interactions between the clusters are weak and hence the sensitivity is stronger. On the other hand, in normal magnets where the interaction between magnetic ions is strong, a very large frequency is required to see any significant shift in ac susceptibility.

The frequency dependence of freezing temperature T_f obtained from the real part of the ac susceptibility is presented in the lower panel of Fig. 7. In SG systems, the frequency dependence of T_f can be described by the standard critical slowing down behavior (power law), given by the dynamic

TABLE I. Parameters obtained from the ac susceptibility analysis using Eqs. (7) and (10).

H (T)	T_g (K)	$z\nu'$	τ^* (sec)	τ_0 (sec)	E_a/k_B (K)	T_0 (K)
0	22.0 ± 0.1	4.2 ± 0.2	$(1.1 \pm 0.6) \times 10^{-10}$	$(6.6 \pm 1.5) \times 10^{-9}$	16.0 ± 0.6	21.1 ± 0.1
0.25	17.8 ± 0.1	4.3 ± 0.2	$(1.6 \pm 0.5) \times 10^{-9}$	$(6.2 \pm 1.6) \times 10^{-8}$	16.4 ± 0.6	16.8 ± 0.2

scaling theory [2,36],

$$\tau = \tau^* \left(\frac{T_f - T_g}{T_g} \right)^{-z\nu'}, \tag{6}$$

where the characteristic time τ describes the dynamical fluctuation time scale and corresponds to the observation time ($t_{obs} = 1/2\pi\nu$), τ^* is the relaxation time of a single spin flip of the fluctuating entities, T_g is the static freezing temperature as ν tends to zero, z is the dynamic critical exponent, and ν' is the critical exponent of the correlation length $\zeta = (T_f/T_g - 1)^{-\nu'}$. The dynamic scaling hypothesis connects τ to ζ as $\tau \sim \zeta^z$.

To fit the data, the power law in Eq. (6) can further be rewritten as

$$\log_{10} \tau = \log_{10} \tau^* - z\nu' \log_{10} \left(\frac{T_f}{T_g} - 1 \right). \tag{7}$$

In the lower left panel of Fig. 7, we have plotted $\log_{10}(\tau)$ versus $\log_{10}(T_f/T_g - 1)$ for $H_{dc} = 0$ and 0.25 T fixing $T_g = 22.0 \pm 0.1$ and 17.8 ± 0.1 K, respectively, obtained via the best fit of the data by the power law [Eq. (6)]. Both the curves show a linear behavior and the obtained parameters, τ^* and $z\nu'$ from a straight line fit [Eq. (7)] are listed in Table I. The dynamic scaling suggests that there is a divergence of the relaxation time at a finite transition temperature, which demonstrates a true phase transition from PM to SG in $Cr_{0.5}Fe_{0.5}Ga$. The parameters τ^* and $z\nu'$ are believed to give more reliable insight into the SG dynamics. For conventional SG systems, the value of $z\nu'$ typically lies between $\sim$4 and $\sim$12, while the value of τ^* ranges from 10^{-10} to 10^{-13} s [14,16,37–39]. Similarly, for the canonical SG and cluster SG, the characteristic range of τ^* varies from $\sim 10^{-12}$ to $\sim 10^{-13}$ s and $\sim 10^{-7}$ to $\sim 10^{-10}$, respectively [2,14,31,39,40]. Clearly, our obtained values of τ^* and $z\nu'$ fall within the ranges reported for typical cluster SG systems [14,16,31,40]. A high value of τ^* also points toward the fact that in $Cr_{0.5}Fe_{0.5}Ga$, spin dynamics occurs in a slow manner, due to the presence of interacting clusters rather than individual spins [31,38]. No significant change in $z\nu'$ was observed, while changing the field from 0 to 0.25 T but the value of τ^* is changed by an order of magnitude, which is still within the range expected for cluster-SG systems.

The presence of interacting clusters is also evident from the failure of Arrhenius law to fit the frequency dependent T_f data. Arrhenius law, which is applicable for noninteracting or weakly interacting magnetic entities can be written as [3]

$$\tau = \tau_0 \exp \left(\frac{E_a}{k_B T_f} \right), \tag{8}$$

where τ_0 has the same physical meaning as τ^* and E_a/k_B is the average activation energy of the relaxation barrier. The activation energy basically measures the energy barrier in which the metastable states are separated and the Arrhenius law accounts for the timescale to overcome the energy barriers by the activation process. Our attempt to estimate τ_0 and E_a/k_B from the linear fit of the $\ln(\tau)$ versus $1/T_f$ data in zero field yields completely unphysical values [$\tau_0 \simeq 2.1 \times 10^{-62}$ s and $E_a/k_B \simeq (3120 \pm 68)$ K]. This failure adds further support to the argument that the dynamics in our system is not simply due to single spin flips, rather it is a cooperative character due to inter-cluster interactions.

Another dynamical scaling law in spin-glass freezing is the phenomenological Vogel-Fulcher (VF) law, which takes into account the interaction among the spins. According to this law, the frequency-dependent T_f can be described by [2,41]

$$\tau = \tau_0 \exp \left[\frac{E_a}{k_B (T_f - T_0)} \right], \tag{9}$$

where T_0 is the empirical VF temperature, which is often interpreted as the interaction strength among the dynamic entities. For the purpose of fitting, it is convenient to rewrite Eq. (9) as

$$\ln \tau = \ln \tau_0 + \frac{E_a/k_B}{(T_f - T_0)}. \tag{10}$$

Here, we show that the variation of T_f in the frequency range, which has been experimentally accessible to us, can be described by this formula. In the lower right panel of Fig. 7, the plot of $\ln \tau$ versus $1/(T_f - T_0)$ is shown, which can be fitted well by Eq. (10) with $T_0 \simeq 21.1$ K and 16.8 K for $H_{dc} = 0$ and 0.25 T, respectively. The parameters, E_a/k_B and τ_0 obtained from the slope and intercept of the linear fit are summarized in Table I. A nonzero value of T_0 and the agreement of VF law with our data suggest a finite interaction among the spins and hence the formation of clusters. The activation energy in the system is expected to be tuned under external magnetic field (H). It is predicted that the magnitude of the spin-glass free energy barriers (E_a/k_B) diminishes as H^2, the coefficient of which is proportional to the number of correlated spins [42,43]. However, our measurements at $H = 0$ and 0.25 T donot yield any visible change in E_a/k_B, which possibly suggests the role of dominant anisotropy in the spin system.

From the above assessment, it is clear that the change of relaxation time τ in our experimental frequency range can be described equally well by both power law [Eq. (7)] and VF law [Eq. (10)]. The obtained value of τ^* from the power law is about an order of magnitude smaller than τ_0 obtained from the VF law. Such difference in characteristic time constant using two dynamical scaling laws are also reported in many cluster-SG systems, e.g., Fe_2O_3 [44], Ni doped $La_{1.85}Sr_{0.15}CuO_4$ [16], etc. Nevertheless, the characteristic time constants (τ^* and τ_0) obtained from both fits fall in the expected range for typical cluster-SG systems. The value of T_g is found to be larger than T_0 only a few percent, in accordance with the

general trend found in the cluster-SG systems [16]. Further, in the frame of the VF model, $T_0 \ll E_a/k_B$ indicates a weak coupling and $T_0 \gg E_a/k_B$ a strong one [45]. For our case, T_0 is about $\sim 1.3 E_a/k_B$ in zero field, which falls in the intermediate regime, suggesting a finite interaction among the magnetic entities. Moreover, the Tholence criterion $\delta T_{Th} = \frac{T_f - T_0}{T_f}$ is also used to compare different SG systems [46]. In our case, the value of δT_{Th} is calculated to be ~ 0.06 [taking $T_f \simeq 22.5$ K and $T_0 \simeq 21.1$ K] at zero field, which is comparable to the value reported for cluster-SG system $PrRhSn_3$ ($\delta T_{Th} \simeq 0.076$) [31].

It is worth mentioning that a qualitative difference is expected between power law and VF law when the measured frequency range is large enough [41]. For instance, the difference is clearly visible for $Cu_{0.954}Mn_{0.046}$ where the variation of τ is over 11 orders of magnitude [41]. Further, closer to T_0 (and T_g), the VF law can be adjusted to match the power law through the relation [41]

$$ln\left(\frac{40k_B T_f}{E_a}\right) \sim \frac{25}{z\nu'}. \tag{11}$$

Using $E_a/k_B \simeq 16$ K, obtained from the VF law and $T_f \simeq 22.5$ K for $\nu = 200$ Hz in Eq. (11), the value of $z\nu'$ was calculated to be ~ 6.2, which is slightly larger than 4.2, obtained directly from the power law fit but within the range expected for cluster-SGs.

E. Nonequilibrium dynamics

1. Magnetic relaxations

Different types of glassy systems are characterized by their magnetic relaxation behavior. To investigate such a behavior, magnetic relaxation measurement was performed at different temperatures ($T = 5$, 10, and 15 K) in the ZFC condition. The sample was cooled under zero applied field from 50 K (PM state) to the desired temperature, which is below T_f. After a waiting time of $t_w = 60$ s, a magnetic field of 200 Oe was applied and the time evolution of magnetization [$M(t)$] was measured. The results are presented in Fig. 8. The $M(t)$ curves follow the standard stretched exponential function

$$M(t) = M_0 - M_g \exp\left[-\left(\frac{t}{\tau}\right)^{\beta}\right], \tag{12}$$

where M_0 is an intrinsic magnetization, M_g is related to a glassy component of magnetization, τ is the characteristic relaxation time constant, and β is the stretching exponent, which has values between 0 and 1 and is a function of temperature only. Although the above function has no specific theoretical justification, it has been widely used to fit the magnetic relaxation data of SG systems [47]. In this relation, $\beta = 0$ implies that $M(t)$ is constant, i.e., no relaxation at all, and $\beta = 1$ implies that the system relaxes with a single time constant. Therefore the value of β covers the dynamics of spins with very strong to no relaxation limit. The value of β depends on the nature of the energy barriers involved in the relaxation. For systems with a distribution of energy barriers, β lies between 0 and 1, whereas for a uniform energy barrier, $\beta = 1$. The value of β obtained from our fit is found to vary from 0.5 to 0.6. These values are within the range (0 to 1) of

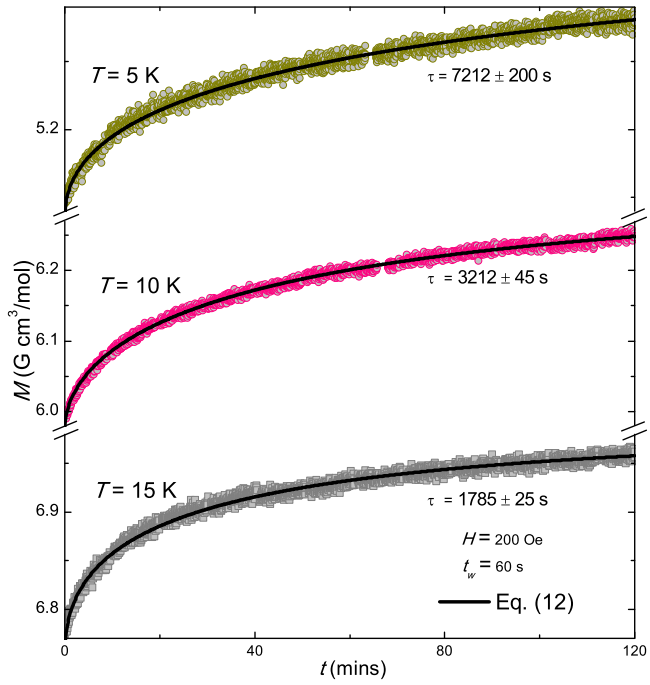

FIG. 8. Relaxation of the zero-field-cooled (ZFC) magnetization measured at different temperatures $T = 5$, 10, and 15 K for a waiting time $t_w = 60$ s, as discussed in the text. The solid lines represent the fit using stretched exponential function given in Eq. (12).

different glassy systems reported earlier [2,14,38,48–51]. Further, $\beta < 1$ signifies that the system evolves through a number of intermediate metastable states, i.e., activation takes place against multiple anisotropic barriers. Moreover, the value of τ is found to increase with decreasing temperature as expected for the glassy systems, below T_f [15,24]. In fact, the values of τ obtained for $Cr_{0.5}Fe_{0.5}Ga$ are almost comparable to that reported for other glassy systems, such as Nd_5Ge_3 (Ref. [24]) and U_2PdSi_3 (Ref. [15]).

2. Magnetic memory effect

In order to examine the presence of nonergodicity in the alloy and to gain new information on the low temperature dynamics, magnetic memory measurements were performed following the FC and ZFC protocols. The results are depicted in Figs. 9(a) and 9(b), respectively. In the FC condition, the sample was cooled down from 50 K (PM state) to 2 K at a constant cooling rate (0.5 K/min) in an applied field of 200 Oe. The cooling process was interrupted at $T_1^{int} = 12$ K and $T_2^{int} = 5$ K for a duration of $t_w = 2$ hours each. During t_w, at each temperature, the magnetic field was switched off and the system was allowed to relax. After each waiting period, the same magnetic field was switched on and the FC process was resumed. The magnetization measured during this process is denoted as M_{FC}^{int} which produces steplike features at 12 and 5 K. After reaching 2 K, the sample was heated under the same field without any interruption and $M(T)$ was recorded up to 50 K, which is designated as M_{FCW}^{mem}. Interestingly, the obtained M_{FCW}^{mem} also exhibits characteristic features at each interruption performed in M_{FC}^{int}, as an attempt to follow the

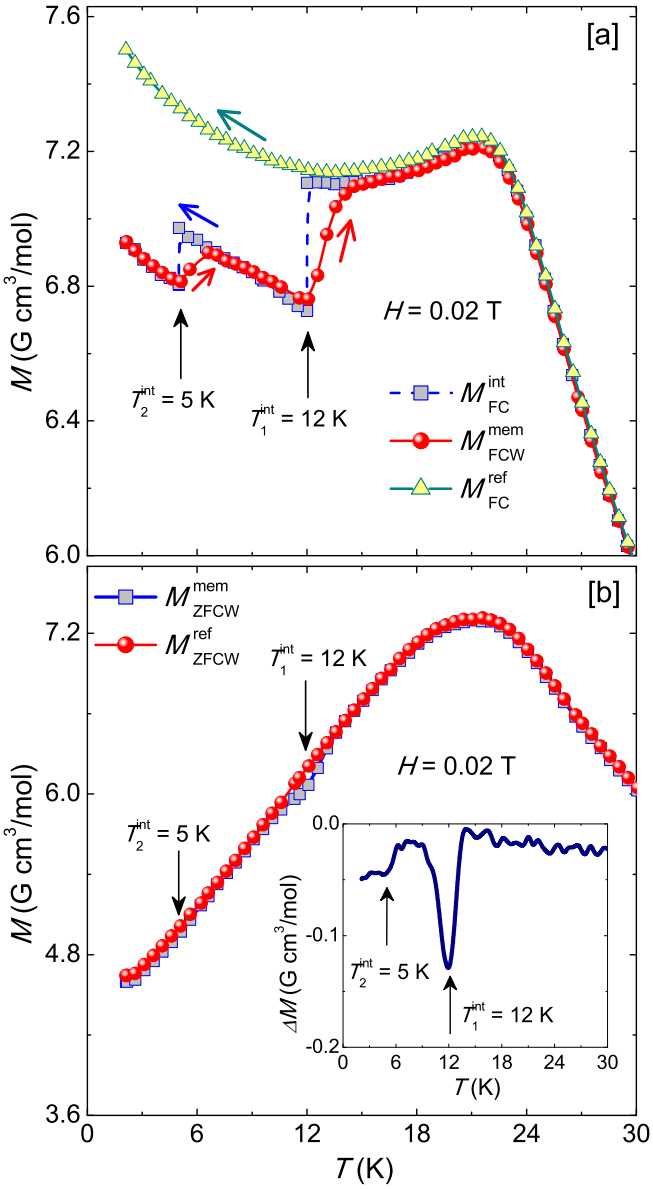

FIG. 9. Memory effect as a function of temperature in (a) FC and (b) ZFC protocols in $H = 200$ Oe, as discussed in the text. The measurements were interrupted at $T_1^{int} = 12$ K and $T_2^{int} = 5$ K for 2 hours each. Inset: Difference in magnetization $\Delta M = (M_{ZFCW}^{mem} - M_{ZFCW}^{ref})$ vs T for the ZFC condition.

past history of the magnetization. Thus it is a clear signature of the magnetic memory in the system. A FC curve (M_{FC}^{ref}) in the same field without any interruption is also measured for reference.

Similar memory effect was also measured in ZFC condition in which the sample was cooled from 50 K (PM state) to 2 K at a constant cooling rate (0.5 K/min) in zero applied field. The cooling was interrupted at $T_1^{int} = 12$ K and $T_1^{int} = 5$ K for $t_w = 2$ hours each. After reaching 2 K, a magnetic field of 200 Oe was applied and $M(T)$ was recorded during warming which is designated as M_{ZFCW}^{mem}. For the sake of completeness, a reference curve was recorded by conventional ZFCW protocol in $H = 200$ Oe, which is represented as M_{ZFCW}^{ref}. These two curves were found to overlap with each

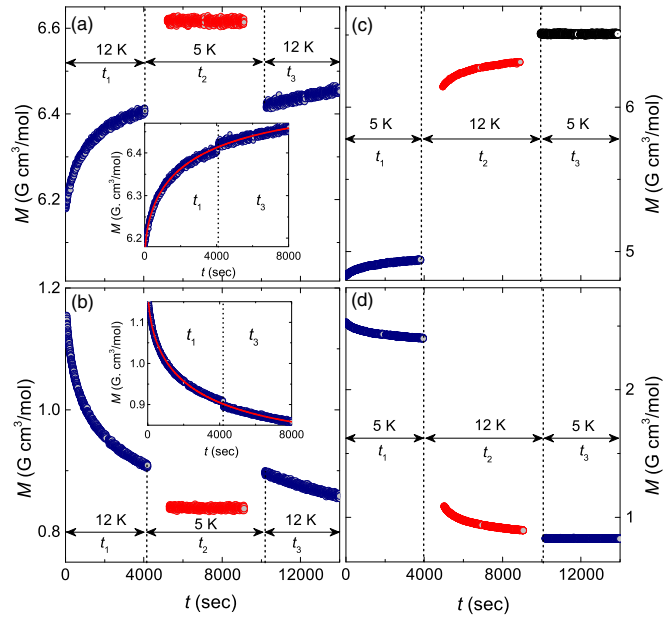

FIG. 10. Magnetic relaxation measurements in the negative T cycle in an applied field of $H = 200$ Oe for (a) ZFC and (b) FC methods. Insets: $M(t)$ data at 12 K for negative FC and ZFC T cycles along with the fit by Eq. (12). For the positive T cycle, ZFC and FC data are shown in (c) and (d), respectively.

other except at the interrupted temperature regions. This is brought out very clearly in the inset of Fig. 9(b) where the difference in magnetization $\Delta M (= M_{ZFCW}^{mem} - M_{ZFCW}^{ref})$ is plotted against temperature. It exhibits memory dips at each interruption points (12 and 5 K). Thus the observation of memory effect in both ZFC and FC conditions strengthens our assessment as cluster-SG behavior of the compound.

To study the memory effect in further details, we performed the relaxation memory measurements for both negative and positive T cycles as discussed below.

Negative T-cycle. The relaxation behavior was recorded for the negative T cycle for both ZFC and FC conditions and the results are shown in Figs. 10(a) and 10(b), respectively. In the ZFC process, the sample was cooled down from 50 to 12 K (below T_f) in zero field. At 12 K, a field of 200 Oe was applied and $M(t)$ was measured for a period of $t_1 = 1$ h. It is found to increase exponentially with t. The sample was further cooled down to 5 K in the same field and again $M(t)$ was measured for $t_2 = 1$ h, which is found to be almost constant with t. Subsequently, the temperature was restored back to 12 K and $M(t)$ was recorded for $t_3 = 1$ h in the same field which again varies exponentially with t. In the FC process, the sample was field cooled down to 12 K in a field of 200 Oe. At 12 K, $M(t)$ was measured for $t_1 = 1$ h after switching off the field and it was found to decay exponentially with t. The sample was further cooled down to 5 K in zero field and $M(t)$ was measured for $t_2 = 1$ h, which is found to be constant with t. Finally, the sample was warmed back to 12 K in zero field and $M(t)$ was recorded again for $t_3 = 1$ hour which again decays exponentially with t.

As shown in the insets of Figs. 10(a) and 10(b), when the $M(t)$ data at 12 K measured during t_1 and t_3 put together, they

simply follow a continuous growth and decay curve for the ZFC and FC processes, respectively. It indicates that the state of the sample before cooling is recovered when the sample is cycled back to the initial temperature. This is a straight forward demonstration of the memory effect in a cluster SG system where the sample remembers its previous state even after experiencing a large change in M. These curves were fitted by the stretched exponential function [Eq. (12)] with $\beta \simeq 0.5$, similar to that observed in the magnetic relaxation measurements.

Positive T-cycle. Similar to the negative T-cycle, both ZFC and FC relaxation behaviours were also recorded for the positive T-cycle and are shown in Figs. 10(c) and 10(d), respectively. In the ZFC process, the sample was cooled down from 50 to 5 K in zero field. At 5 K, a field of 200 Oe was applied and $M(t)$ was recorded for $t_1 = 1$ h, which shows a gradual increase with t. The sample was then heated upto 12 K in the same field and again $M(t)$ was measured for $t_2 =$ 1 h, which also shows a gradual increase with t. Finally, the temperature was restored back to 5 K but the $M(t)$ measured for another $t_3 = 1$ h is found to be t independent. In the FC process, the sample was cooled down to 5 K in a field of 200 Oe. At 5 K, magnetic field was switched off and the same sequence (as for the ZFC process) was repeated. As shown in Fig. 10(d), the obtained results follow the same trend as for the ZFC sequence but in the opposite direction. It is evident that unlike the negative T cycle, there is no continuity in the $M(t)$ data measured during t_1 and t_3 at 5 K suggesting that the nature of the magnetic relaxation during t_3 is quite different from that during t_1. Thus positive T cycling revives the magnetic relaxation process and no magnetic memory effect is observed when the temperature is restored.

The memory effect in SG systems has been widely studied via magnetization measurements. This phenomena is usually discussed in the framework of two theoretical models: the droplet model [6] and the hierarchical model [52]. These are two well established models which are successfully applied in several experimental studies [14,53]. At a given temperature, a multivalley spin structure is organized on the free-energy landscape in the hierarchical model, whereas in the droplet model only one spin configuration is favoured. Basically, in the hierarchical model, these free energy valleys which are metastable states split into new subvalleys as the temperature is lowered and get merged with increasing temperature. This picture obviously give rise to the observed memory effects. When the temperature of the system is lowered from T to $T - \Delta T$, each valley splits into a set of subvalleys. If ΔT is large, the energy barriers separating the main valleys become too high and the system cannot overcome these barriers during the waiting time t_2. Therefore the relaxation occurs only within the subvalleys of each set. As the temperature is brought back to T, the subvalleys and barriers merge back to the original free-energy landscape and the relaxation at T is not at all disturbed by the intermediate relaxations at $T - \Delta T$. However, when the temperature of the system is increased from T to $T + \Delta T$, the barriers between the free energy multi valleys are lowered or even get merged. Therefore the relaxations can occur within different valleys. When the temperature is lowered back to T, although the free-energy landscape is restored, the relative occupancy of each valley does not remain the same as before. Thus the state of the system changes after a temporary heating cycle showing no memory effect.

Experimentally, these two models can be distinguished by studying the influence of T cycling on magnetic relaxation. In the droplet model, the original spin configuration is restored after a T cycling, i.e., one would expect a symmetric behavior in magnetic relaxation with respect to the positive/negative T cycling. On the other hand, in the hierarchical model, the original spin configuration is destroyed after a positive T cycling and one would expect an asymmetric response (or, no memory effect) in magnetic relaxation. Thus, based on the above criteria, our observed asymmetric response in the positive T cycle during both ZFC and FC processes supports the hierarchical organization of the metastable states in the cluster-SG system. Since the hierarchical organization requires a large number of degrees of freedom to be coupled, it can not be produced simply by the independent behavior of individual spins and consequently highlights the important role played by interparticle/intracluster interactions.

IV. SUMMARY

In summary, we present a detailed and a systematic study of the structural and magnetic properties of $Cr_{0.5}Fe_{0.5}Ga$. No evidence of any structural disorder was found from the temperature dependent powder XRD measurements down to 15 K. The temperature dependent dc magnetization shows the onset of a SG transition at low temperatures which is caused by magnetic site disorder and magnetic frustration due to competing AFM and FM interactions. The SG transition is further justified by ac susceptibility measurements. The results clearly indicate that the fitted parameters, as obtained from the relative shift in T_f and the dynamical scaling laws, are consistent with that expected for cluster SG systems. The activation energy of the metastable states is estimated to be $E_a/k_B \simeq 16$ K. A clear signature of the magnetic memory effect was observed below the freezing temperature in both FC and ZFC processes further demonstrating the cluster-SG behavior of the compound under investigation. In the positive T cycle, a small heating reinitializes the relaxation process and the magnetization is unable to restore its initial value. Such an asymmetric response of magnetic relaxation with respect to positive temperature change favours the hierarchical model. The Debye temperature estimated from the low temperature $C_p(T)$ data is consistent with that obtained from the $V_{cell}(T)$ analysis. Although our experimental results point towards the formation of cluster SG state, the underlying mechanism behind such a formation is not yet understood. Further studies, preferably neutron scattering and μSR experiments, may provide useful insight.

ACKNOWLEDGMENTS

We would like to acknowledge BRNS, India for financial support bearing sanction No.37(3)/14/26/2017-BRNS. We thanks B. R. Sekhar for his valuable suggestions. P.B. is supported by the IISER-TVM post-doctoral fellowship programme.

[1] K. Fisher and J. Hertz, *Spin Glasses*, Cambridge Studies in Magnetism (Cambridge University Press, Cambridge, England, 1991).

[2] J. A. Mydosh, *Spin Glasses: An Experimental Introduction* (Taylor & Francis, London, 1993).

[3] K. Binder and A. P. Young, Rev. Mod. Phys. **58**, 801 (1986).

[4] M. Weissman, Rev. Mod. Phys. **65**, 829 (1993).

[5] K. Jonason, E. Vincent, J. Hammann, J. P. Bouchaud, and P. Nordblad, Phys. Rev. Lett. **81**, 3243 (1998).

[6] D. S. Fisher and D. A. Huse, Phys. Rev. B **38**, 373 (1988).

[7] S. Karmakar, S. Taran, E. Bose, B. K. Chaudhuri, C. Sun, C. L. Huang, and H. D. Yang, Phys. Rev. B **77**, 144409 (2008).

[8] S. Chatterjee, S. Giri, S. K. De, and S. Majumdar, Phys. Rev. B **79**, 092410 (2009).

[9] J. Souletie, J. Phys. (Paris) **39**, C2-3 (1978).

[10] J. S. Gardner, M. J. P. Gingras, and J. E. Greedan, Rev. Mod. Phys. **82**, 53 (2010).

[11] O. Gourdon, S. L. Bud'ko, D. Williams, and G. J. Miller, Inorg. Chem. **43**, 3210 (2004).

[12] H. Ko, O. Gourdon, D. Gout, E.-D. Mun, S. Thimmaiah, and G. J. Miller, Inorg. Chem. **49**, 11505 (2010).

[13] J. Rodríguez-Carvajal, Phys. B Condens. Matter **192**, 55 (1993).

[14] S. Pakhira, C. Mazumdar, R. Ranganathan, S. Giri, and M. Avdeev, Phys. Rev. B **94**, 104414 (2016).

[15] D. X. Li, Y. Shiokawa, Y. Homma, A. Uesawa, A. Dönni, T. Suzuki, Y. Haga, E. Yamamoto, T. Honma, and Y. Ōnuki, Phys. Rev. B **57**, 7434 (1998).

[16] A. Malinowski, V. L. Bezusyy, R. Minikayev, P. Dziawa, Y. Syryanyy, and M. Sawicki, Phys. Rev. B **84**, 024409 (2011).

[17] R. Nath, A. A. Tsirlin, H. Rosner, and C. Geibel, Phys. Rev. B **78**, 064422 (2008).

[18] M. Gabay and G. Toulouse, Phys. Rev. Lett. **47**, 201 (1981).

[19] J. De Almeida and D. J. Thouless, J. Phys. A: Math. Gen. **11**, 983 (1978).

[20] A. P. Malozemoff, S. E. Barnes, and B. Barbara, Phys. Rev. Lett. **51**, 1704 (1983).

[21] D. Li, S. Nimori, Y. Shiokawa, A. Tobo, H. Onodera, Y. Haga, E. Yamamoto, and Y. Ōnuki, Appl. Phys. Lett. **79**, 4183 (2001).

[22] D. X. Li, S. Nimori, Y. Shiokawa, Y. Haga, E. Yamamoto, and Y. Onuki, Phys. Rev. B **68**, 172405 (2003).

[23] T. Chakrabarty, A. V. Mahajan, and S. Kundu, J. Phys.: Conden. Matter. **26**, 405601 (2014).

[24] B. Maji, K. Suresh, and A. Nigam, J. Phys.: Conden. Matter. **23**, 506002 (2011).

[25] X. K. Zhang, J. J. Yuan, Y. M. Xie, Y. Yu, F. G. Kuang, H. J. Yu, X. R. Zhu, and H. Shen, Phys. Rev. B **97**, 104405 (2018).

[26] B. Barbara, A. P. Malozemoff, and Y. Imry, Phys. Rev. Lett. **47**, 1852 (1981).

[27] B. Dieny and B. Barbara, Phys. Rev. Lett. **57**, 1169 (1986).

[28] Y. Tabata, T. Waki, and H. Nakamura, Phys. Rev. B **96**, 184406 (2017).

[29] P. M. Shand, T. Rash, M. Streicher, T. E. Kidd, K. R. Boyle, and L. H. Strauss, Phys. Rev. B **82**, 214413 (2010).

[30] F. Wang, J. Zhang, Y.-f. Chen, G.-j. Wang, J.-r. Sun, S.-y. Zhang, and B.-g. Shen, Phys. Rev. B **69**, 094424 (2004).

[31] V. K. Anand, D. T. Adroja, and A. D. Hillier, Phys. Rev. B **85**, 014418 (2012).

[32] E. S. R. Gopal, *Specific Heats at Low Temperatures* (Springer, Boston, MA, 2012).

[33] C. Tien, C. H. Feng, C. S. Wur, and J. J. Lu, Phys. Rev. B **61**, 12151 (2000).

[34] C. A. M. Mulder, A. J. van Duyneveldt, and J. A. Mydosh, Phys. Rev. B **25**, 515 (1982).

[35] J. A. Mydosh, Rep. Prog. Phys. **78**, 052501 (2015).

[36] P. C. Hohenberg and B. I. Halperin, Rev. Mod. Phys. **49**, 435 (1977).

[37] D. N. H. Nam, R. Mathieu, P. Nordblad, N. V. Khiem, and N. X. Phuc, Phys. Rev. B **62**, 8989 (2000).

[38] S. Ghara, B.-G. Jeon, K. Yoo, K. H. Kim, and A. Sundaresan, Phys. Rev. B **90**, 024413 (2014).

[39] J. Lago, S. J. Blundell, A. Eguia, M. Jansen, and T. Rojo, Phys. Rev. B **86**, 064412 (2012).

[40] T. Mori and H. Mamiya, Phys. Rev. B **68**, 214422 (2003).

[41] J. Souletie and J. L. Tholence, Phys. Rev. B **32**, 516(R) (1985).

[42] S. Guchhait and R. L. Orbach, Phys. Rev. Lett. **118**, 157203 (2017).

[43] Q. Zhai, D. C. Harrison, and R. L. Orbach, Phys. Rev. B **96**, 054408 (2017).

[44] M. D. Mukadam, S. M. Yusuf, P. Sharma, S. K. Kulshreshtha, and G. K. Dey, Phys. Rev. B **72**, 174408 (2005).

[45] S. Shtrikman and E. Wohlfarth, Phys. Lett. A **85**, 467 (1981).

[46] J.-L. Tholence, Physica B **126**, 157 (1984).

[47] R. V. Chamberlin, G. Mozurkewich, and R. Orbach, Phys. Rev. Lett. **52**, 867 (1984).

[48] D. Chu, G. G. Kenning, and R. Orbach, Phys. Rev. Lett. **72**, 3270 (1994).

[49] C. A. Cardoso, F. M. Araujo-Moreira, V. P. S. Awana, E. Takayama-Muromachi, O. F. de Lima, H. Yamauchi, and M. Karppinen, Phys. Rev. B **67**, 020407 (2003).

[50] N. Khan, P. Mandal, and D. Prabhakaran, Phys. Rev. B **90**, 024421 (2014).

[51] A. Bhattacharyya, S. Giri, and S. Majumdar, Phys. Rev. B **83**, 134427 (2011).

[52] F. Lefloch, J. Hammann, M. Ocio, and E. Vincent, Europhys. Lett. **18**, 647 (1992).

[53] Y. Sun, M. B. Salamon, K. Garnier, and R. S. Averback, Phys. Rev. Lett. **91**, 167206 (2003).